Engineered atomically dispersed cobalt sites in one-dimensional pyridine-based covalent organic frameworks for enhanced photocatalytic CO_2 reduction

Siting Ma [a], Zijie Fu [a], Chenxi Sun [a], Ying Ha [c], Xiaohong Yin [a, b], Manman Mu [a, b, *], Guoyi Bai [a, b, *]

[a] *School of Chemistry and Chemical Engineering, Tianjin University of Technology, Tianjin, 300384, PR China*

[b] *Tianjin Key Laboratory of Organic Solar Cells and Photochemical Conversion, Tianjin, 300384, PR China*

[c] *School of Environmental Science and Engineering, Tianjin University, Tianjin, 300350, PR China*

*Corresponding author:

E-mail address: mu2020@email.tjut.edu.cn (M. Mu)

baiguoyi@hotmail.com (G. Bai)

Contents

1. Experimental section

1.1. Materials

All chemicals and reagents were of analytical grade and used as received without further purification. Tetrakis(4-aminophenyl)ethene (ETTA, 97%), 2, 9-bis[p-(formyl)phenyl]-1, 10-phenanthroline (Phen-COF, 98%), 2, 6-pyridinedicarboxaldehyde (Py, 98%) were purchased from Shanghai Bide Pharmaceutical Technology Co., Ltd. 1,3-dimethyl-2-phenyl-2,3-dihydro-1H-benzo[d]imidazole (BIH, 98%) was supplied by Beijing Innochem Technology Co., Ltd. 1, 2-dichlorobenzene (AR), 1-butanol (AR), tetrahydrofuran (THF, AR), acetic acid, cobalt acetate and ethanol were supplied by Maclin Chemicals.

1.2. Synthesis of 1D Phen-COF

A Pyrex glass tube was charged with tetrakis(4-aminophenyl)ethene (ETTA, 15.7 mg, 0.04 mmol), 2, 9-bis[p-(formyl)phenyl]-1, 10-phenanthroline (Phen, 31.07 mg, 0.08 mmol), 1 mL of 1, 2-dichlorobenzene and 1 mL of 1-butanol. The mixture was sonicated for 10 min, followed by the addition of 0.02 mL of 6M acetic acid. After degassed *via* three freeze-pump-thaw cycles, the tube was sealed and heated at 120℃ for 3 days. The precipitate was collected by centrifugation, washed with ethanol several times and then suspended in tetrahydrofuran (THF) at 60℃ for 3 h. The yellow solid was collected and dried at 60℃ overnight to afford 1D Phen-COF.

1.3. Synthesis of 1D Py-COF

A Pyrex glass tube was charged with ETTA (15.7 mg, 0.04 mmol), 2, 6-pyridinedicarboxaldehyde (Py, 10.81 mg, 0.08 mmol), 1 mL of 1, 2-dichlorobenzene and 1 mL of 1-butanol. The mixture was sonicated for 10 min, followed by the addition of 0.02 mL of 6M acetic acid. After degassed via three freeze-pump-thaw cycles, the tube was sealed and heated at 120℃ for 3 days. The precipitate was collected by centrifugation, washed with ethanol several times and then suspended in THF at 60℃

for 3 h. The yellow solid was collected and dried at 60℃ overnight to obtain 1D Py-COF.

1.4. Synthesis of Co-Phen-COF and Co-Py-COF

1D Py-COF (or 1D Phen-COF, 20 mg) was dispersed in methanol (20 mL) containing cobalt acetate (20 mg). The above mixture was heated at 60℃ for 6 h and then the solid was centrifugated, washed with ethanol and water several times, and then dried under vacuum at 60 ℃ overnight to yield Co-Py-COF (or Co-Phen-COF).

1.5. Photocatalytic CO_2 reduction experiments

The photocatalytic CO_2 reduction experiments were performed in a 50 mL homemade quartz reactor at ambient temperature and atmospheric pressure. Specifically, 20 mg of photocatalyst was dispersed into 20 mL of acetonitrile (CH_3CN) containing 1, 3-dimethyl-2-phenyl-2,3-dihydro-1H-benzo[d]imidazole (BIH, 30 mg), and the mixture was ultrasonicated for 10 minutes to form a suspension. Prior to irradiation, the reaction system was purged with high-purity CO_2 for 30 minutes to remove air. A 300 W Xenon Lamp (PLS-SXE 300, Perfectlight, Beijing) equipped with a UV-cutoff filter ($\lambda \geq 420$ nm, light intensity =1850 $\mu W \cdot cm^{-2}$) served as the light source. The sealed reactor was irradiated for 5 hours with continuous stirring. Gas products were detected on a gas chromatography (GC-99790II, Fuli Co. Ltd., China) equipped with a thermal-conductive detector (TCD) to analyze H_2 and O_2, and flame-ionization detector (FID) to analyze CO and CH_4. A series of control experiments were carried out without photocatalyst, light, sacrificial agent or under N_2 atmosphere to elucidate the key factors influencing photocatalytic CO_2 reduction.

The recycling measurements were conducted and repeated for four times. After each reaction, the catalyst was recovered by centrifugation, washed with water and acetone, and then dried at 60°C under vacuum before be reused in the cycling experiments.

1.6. Characterization methods

1.6.1. Instruments and characterization

Powder X-ray diffraction (PXRD) measurement was conducted on Rigaku, U1 with Cu Kα radiation (λ= 0.15418 Å) operating at 40 kV and 40 mA. Fourier transform infrared (FT-IR) spectra were recorded on a Thermo Scientific Nicolet iS10 instrument ranging from 4000 to 400 cm^{-1}. Scanning electron microscopy (SEM) images were obtained on Merlin Compact. Transmission electron microscopy (TEM) images were obtained on Talos F200X microscopes (FEI Corp.) equipped with an energy-dispersive X-ray (EDX) detector. Nitrogen adsorption and desorption isotherms were measured at 77K by an ASAP 2020 apparatus (Micrometrics Corp.). Surface areas were calculated based on Brunauer-Emmett-Teller (BET) method and the pore size distribution curves were obtained by non-local density functional theory (NLDFT) method. The carbon dioxide isotherms were tested at 298 K. X-ray photoelectron spectroscopy (XPS) and in situ XPS measurements were performed on a ESCALAB250Xi instrument (Thermo Scientific Corp.). X-ray Absorption Near Edge Structure (XANES) spectra were recorded using Rapid 2M (Anhui Absorption Spectroscopy Analysis Instrument Co., Ltd). Co K-edge Extended X-ray Absorption Fine Structure (EXAFS) absorption were recorded in transmission mode. The XAFS spectra of the standard samples (Co foil, CoPc, CoO and Co_3O_4) were recorded in transmission mode. To obtain the quantitative structural parameters around central atoms, data processing was carried out using Athena and Artemis software of the IFEFFIT packages. UV-vis diffuse reflectance spectroscopy (UV-vis DRS) was conducted on a Shimadzu UV-2550 Spectrometer with $BaSO_4$ as the reference. Steady-state Photoluminescence (PL) spectra were recorded on a RiLiF-7000 measurement. Time-resolved PL spectra were performed on Edinburgh FLS1000 spectrophotometer. Inductively coupled plasma-optical emission spectrometry (ICP-OES) was carried out on an Thermo Scientific iCAP RQ instrument.

1.6.2. Photoelectrochemical measurements

Photoelectrochemical measurements were conducted on a CHI 760E electrochemical workstation with a three-electrode system in a 0.5 M Na_2SO_4

electrolyte solution. A saturated Ag/AgCl electrode and Pt wire were used as the reference and counter electrodes, respectively. The catalyst-coated indium-doped tin oxide (ITO) was used as working electrode and the working electrode was fabricated as follows: 5 mg catalyst was dispersed into 250 μL ethanol and 750 μL water containing 50 μL Nafion solution. The mixture was ultrasonically dispersed for 30 min and 100 μL mixture was uniformly dropped on FTO glass (1×1 cm^2) and dried at room temperature. The transient photocurrent responses were recorded in 0.5 M Na_2SO_4 electrolyte using a 300 W xenon lamp. Mott-schottky measurements are tested at specific frequencies of 800 and 1000 Hz. Electrochemical impedance measurements were recorded at open circuit voltage and the frequency range was 1 to 105 Hz with the amplitude at 5 mV.

1.6.3. *In-situ* diffuse reflectance infrared Fourier transform spectroscopy

In-situ diffuse reflectance infrared Fourier transform spectroscopy (DRIFTS) were recorded on a Nicolet iS10 spectrometer equipped with a mercury cadmium telluride detector. The reaction chambers used kHVC-DRP-5 equipped with two KBr windows and a quartz window. First, the sample was treated at 200℃ under N_2 (50 mL min^{-1}) to remove adsorbed contaminants before the measurement. After cooled down to room temperature, the background spectrum was collected by continuous flow of CO_2 gas into the reaction chamber for 0.5 h. Then, the catalyst was exposed to 5 % CO_2 gas and H_2O vapor for 0.5 h, after which the gas was desorbed and irradiated with a whit LED lamp, recording spectrum at intervals.

1.7. Calculation details

The theoretical calculations were carried out by density function theory (DFT) calculations in Vienna *ab initio* simulation package (VASP). Exchange-correlation functionals were described by generalized gradient approximation (GGA) with the Perdew-Burke-Ernzerhof (PBE) pseudopotential. The truncation energy for plane wave were set to 450 eV and the Brillouin zone of supercells was set as 1 × 1 × 3 grid of *k*-points. The convergence criterion for structure optimization was set to: an energy tolerance on each atom of 1 × 10^{-5} eV, and a maximum force tolerance of -0.02 eV/Å.

The lowest unoccupied molecular orbital (LUMO) and the highest occupied molecular orbital (HOMO) were calculated by VASP to analyze the strength of oxidation and reduction.

The free energy changes (ΔG) for each elementary step in the CO_2 reduction and H_2 evolution were calculated as following:

$$\Delta G = \Delta E + \Delta E_{ZPE} - T\Delta S$$

where ΔE is the computed reaction energy, ΔE_{ZPE} and ΔS are the zero-point energy change and the entropy difference between the absorbed state and gas phase, respectively, and T (set to 298.15 K) is the system temperature.

2. Results and Discussion

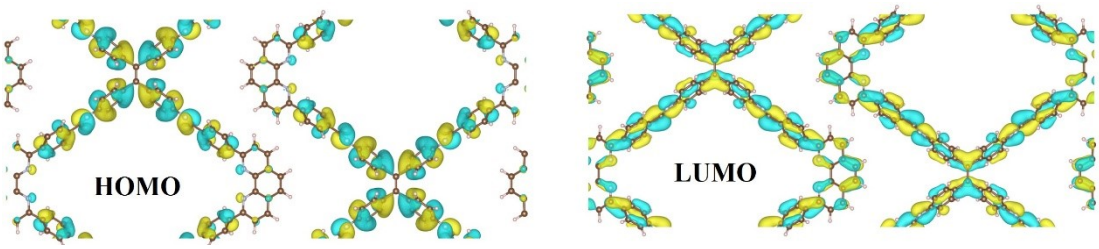

Fig. S1. Calculated HOMO-LUMO distribution of Phen-COF.

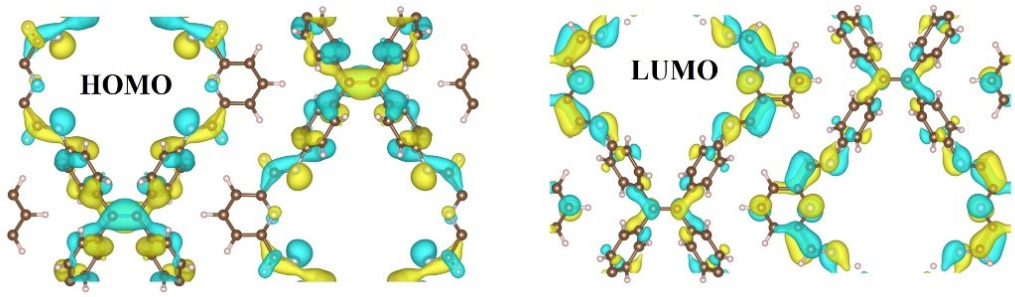

Fig. S2. Calculated HOMO-LUMO distribution of Py-COF.

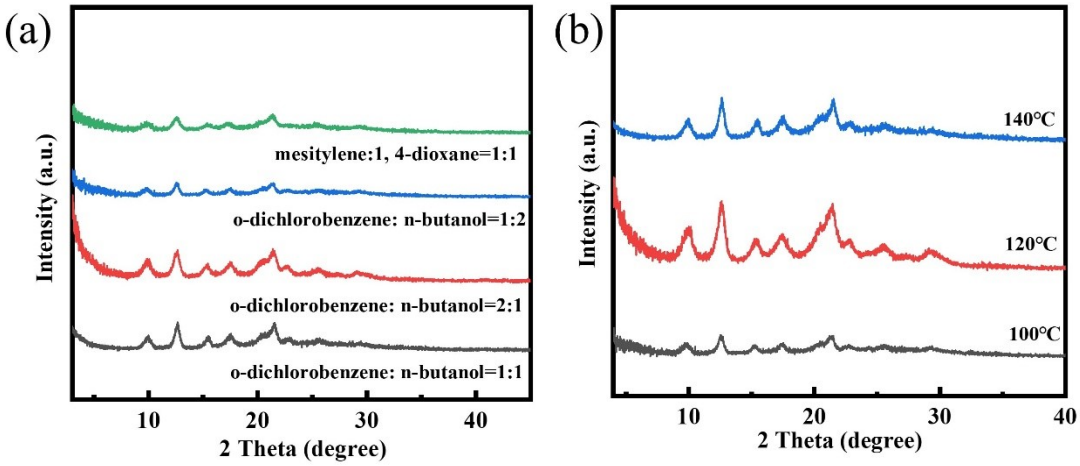

Fig. S3. XRD patterns of Py-COF at (a) solvent compositions and (b) reaction temperatures (100, 120, 140°C) in optimized mixed solvents.

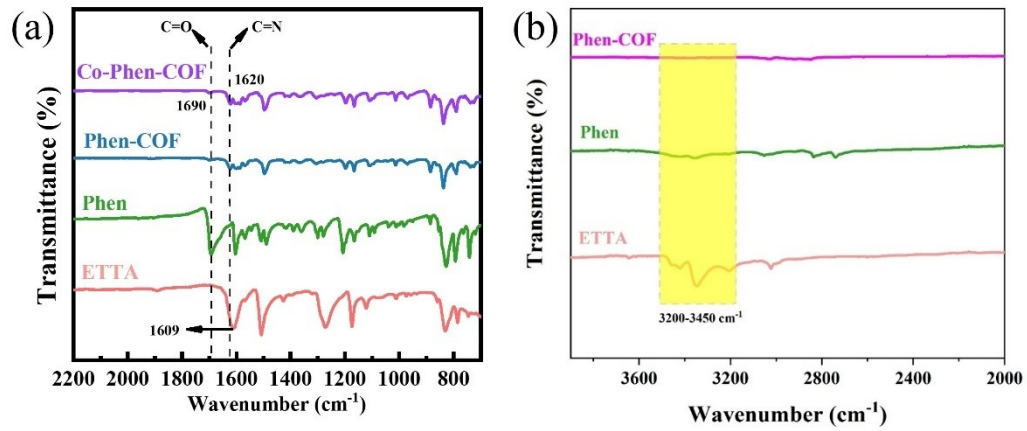

Fig. S4. FT-IR spectra of (a) Phen-COF, Co-Phen-COF and its monomer, (b) ETTA, Phen, and Phen-COF in the range of 3900-2000 cm^{-1}.

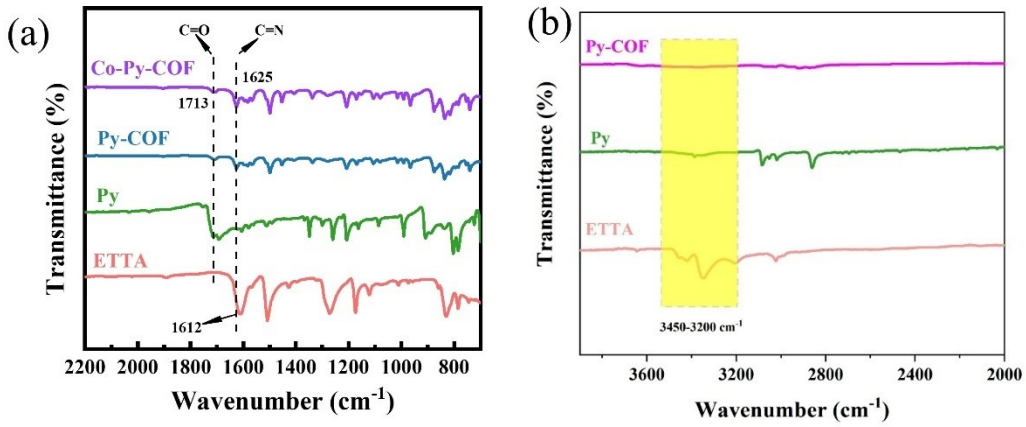

Fig. S5. FT-IR spectra of (a) Py-COF, Co-Py-COF and its monomer, (b) ETTA, Py, and Py-COF in the range of 3900-2000 cm^{-1}.

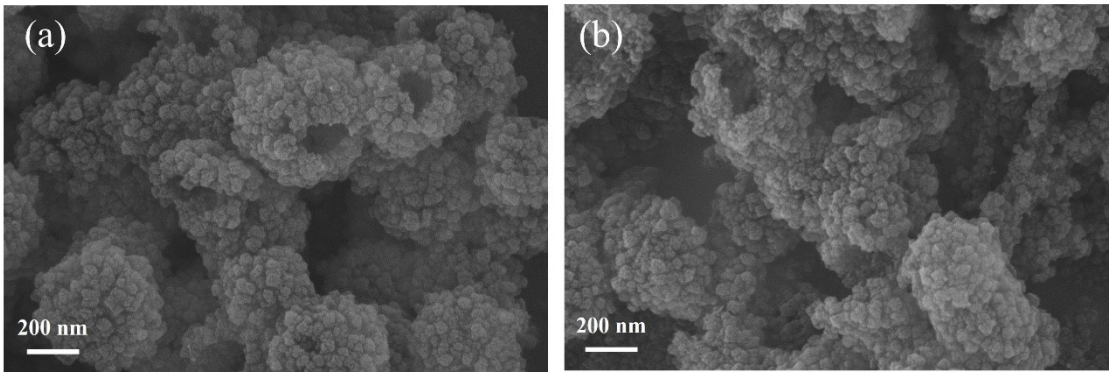

Fig. S6. SEM images of (a) Phen-COF, (b) Co-Phen-COF.

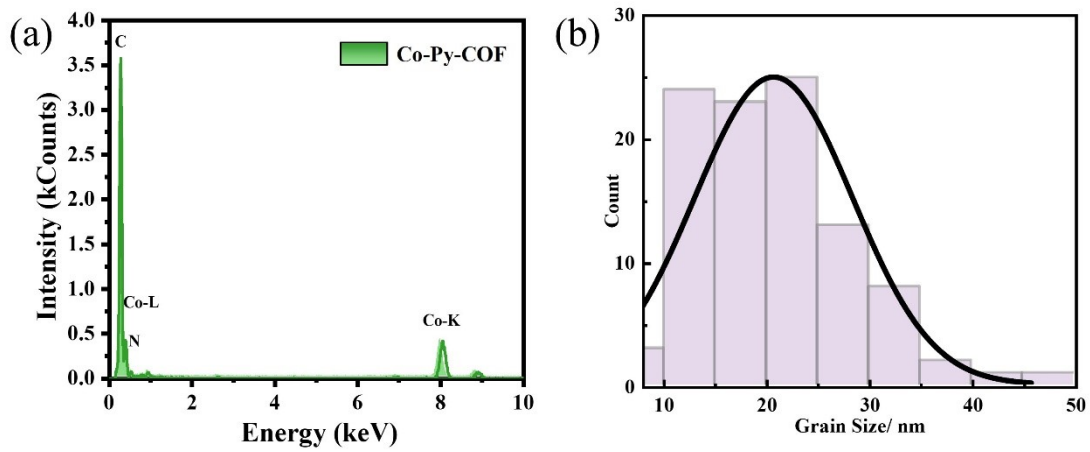

Fig. S7. (a) TEM-EDX spectrum and (b) grain size distribution of Co-Py-COF.

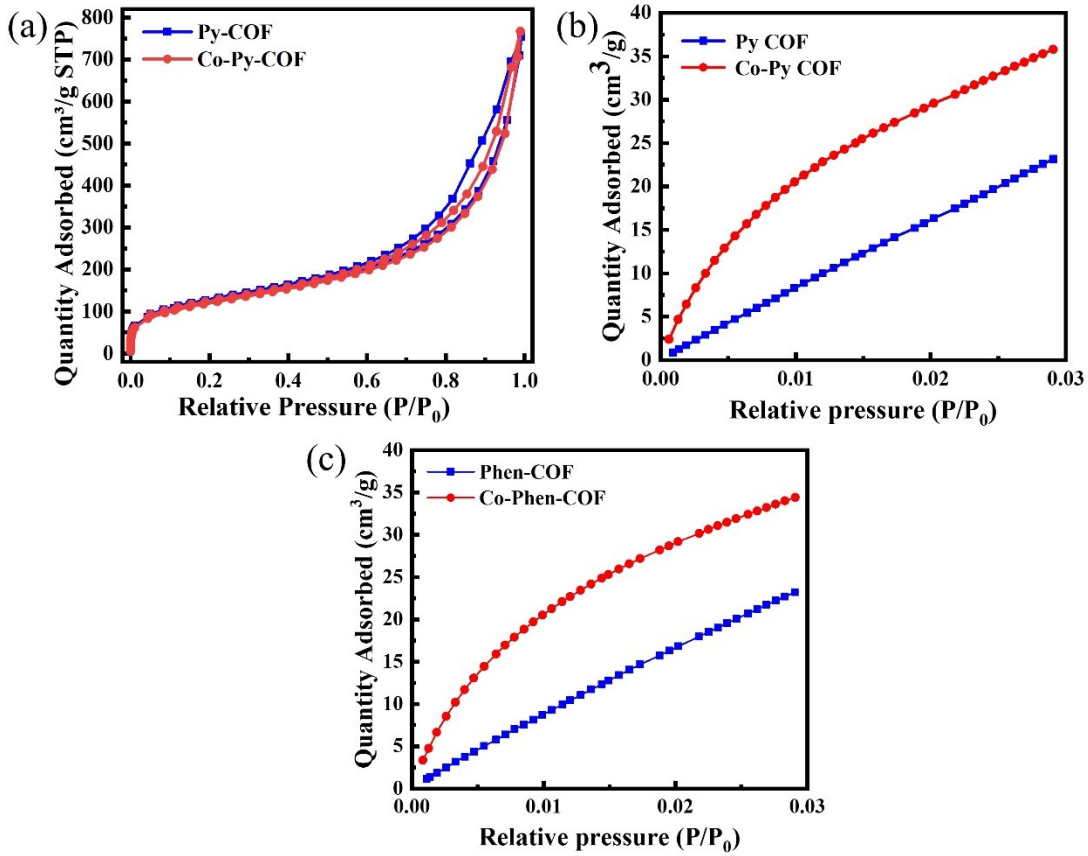

Fig. S8. (a) N_2 adsorption-desorption isotherm of Py-COF and Co-Py-COF, CO_2 sorption isotherms of (b) Py-COF, Co-Py-COF and (c) Phen-COF, Co-Phen-COF at 298K.

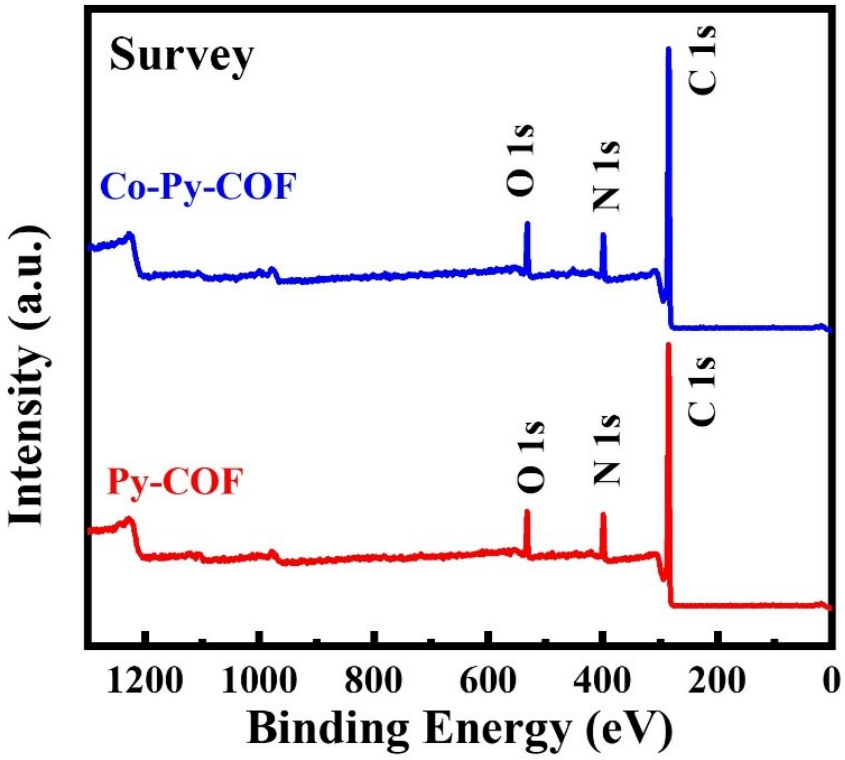

Fig. S9. Survey XPS spectra of Py-COF and Co-Py-COF.

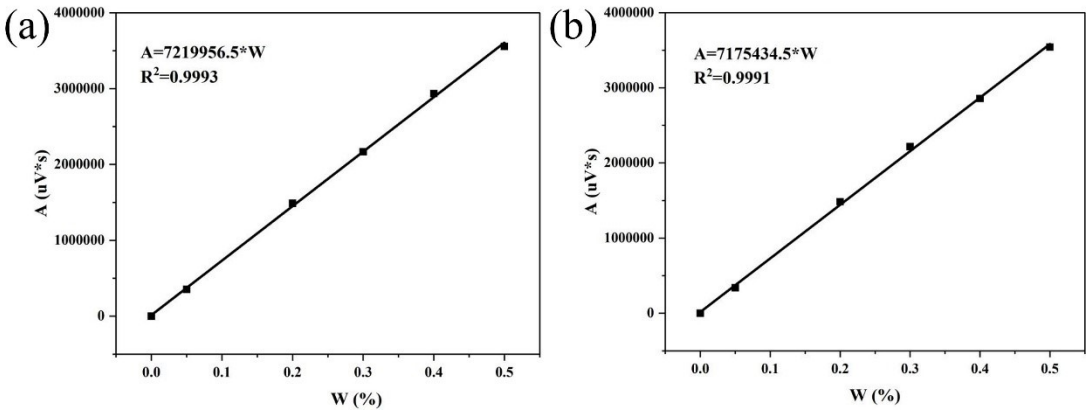

Fig. S10. The standard curves for (a) CO and (b) CH_4.

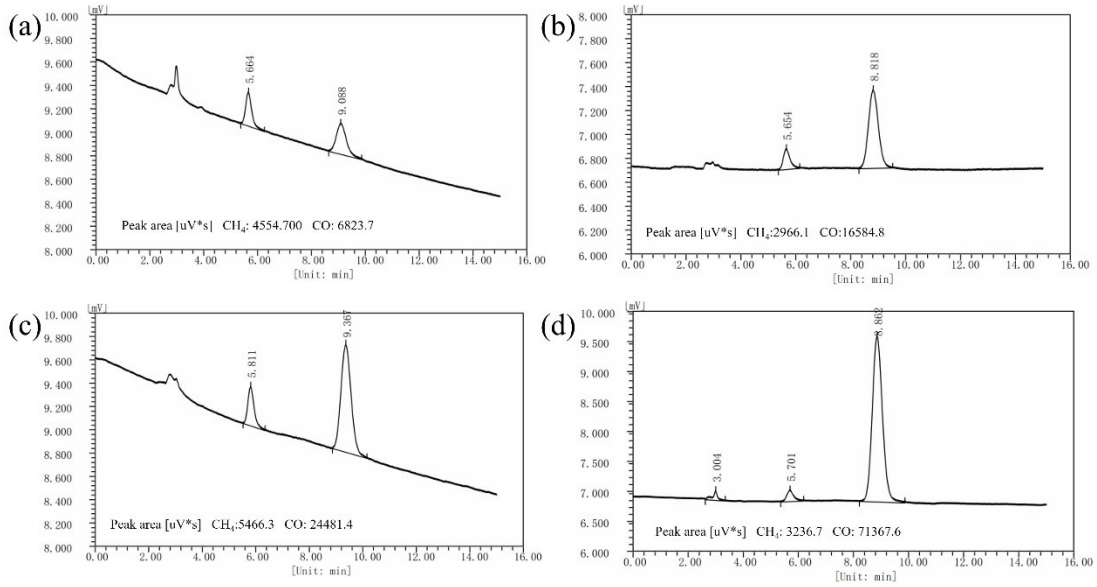

Fig. S11. the gas chromatography data of production rates over (a) Phen-COF, (b) Py-COF, (c) Co-Phen-COF, and (d) Co-Py-COF.

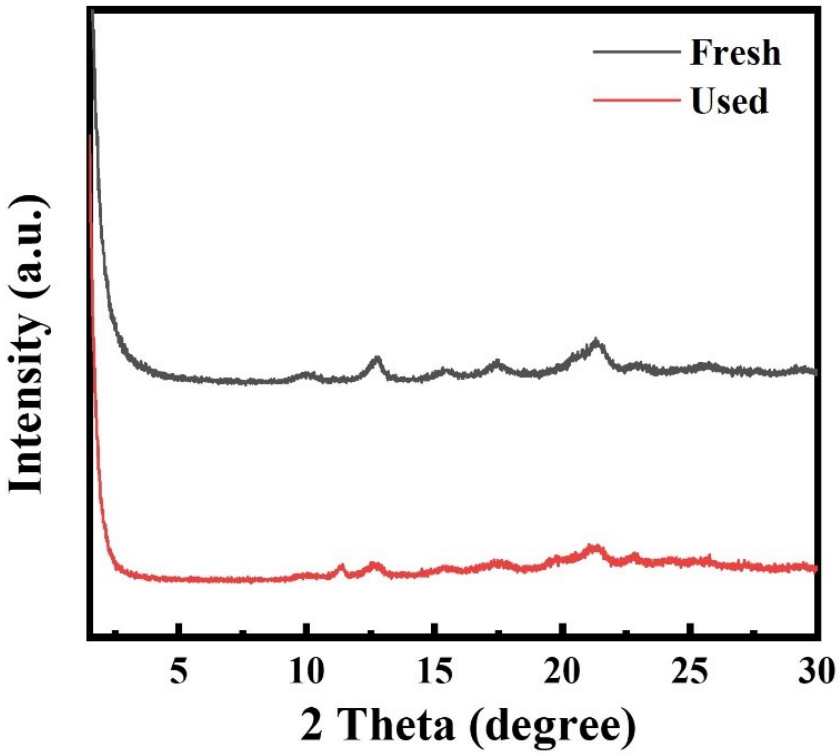

Fig. S12. XRD patterns of the fresh and used Co-Py-COF after the photocatalytic reaction.

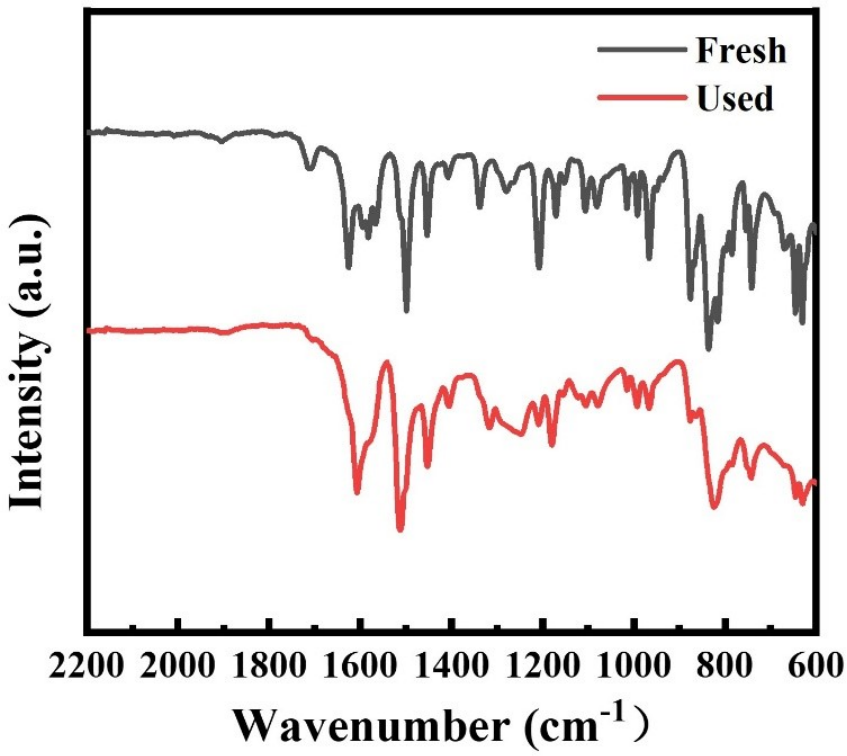

Fig. S13. FT-IR spectra of the fresh and used Co-Py-COF after the photocatalytic reaction.

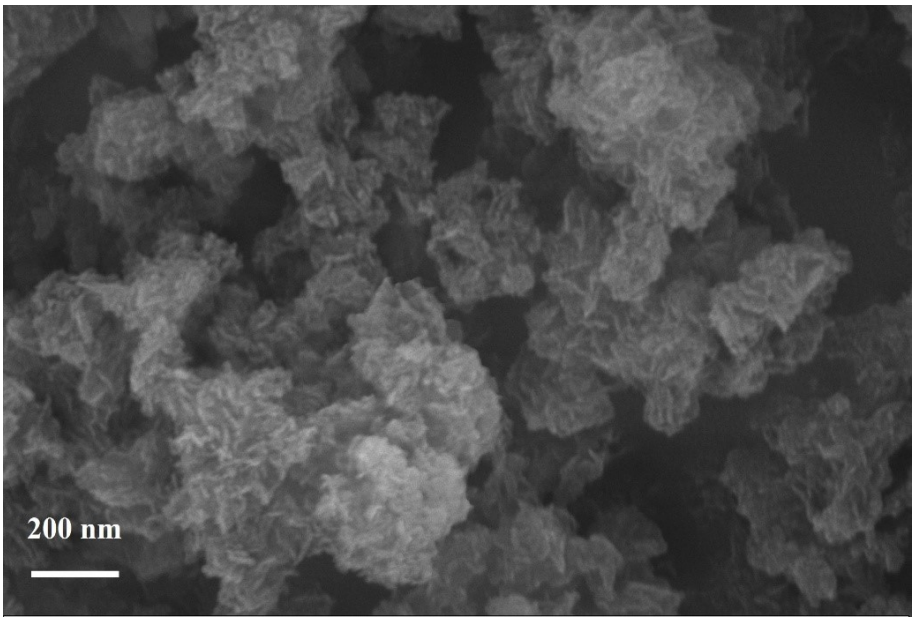

Fig. S14. SEM image of the used Co-Py-COF after the photocatalytic reaction.

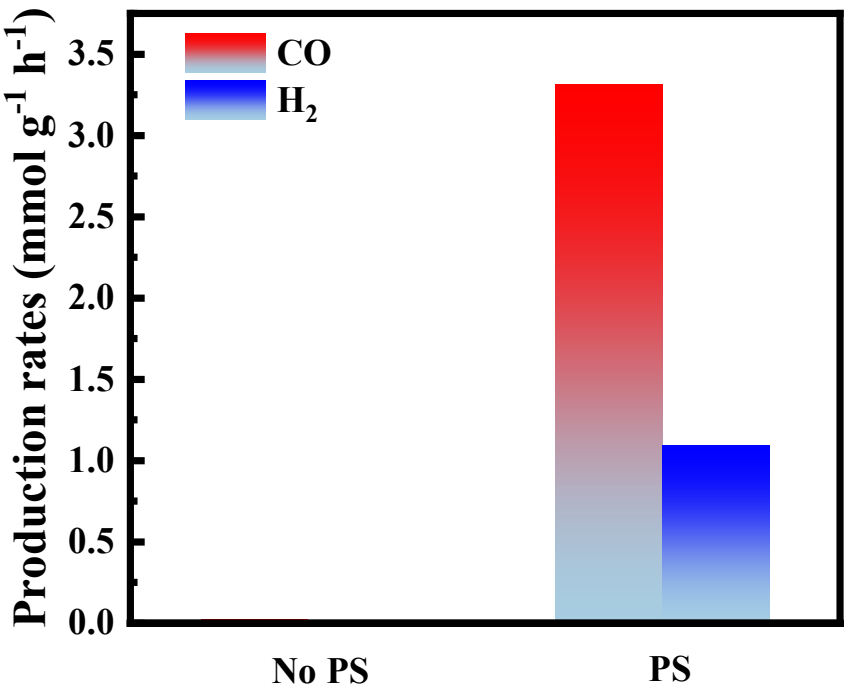

Fig. S15. Production rate of CO and H_2 over Co-Py-COF with or without $Ru(bpy)_3Cl_2$ as photosensitizer (PS).

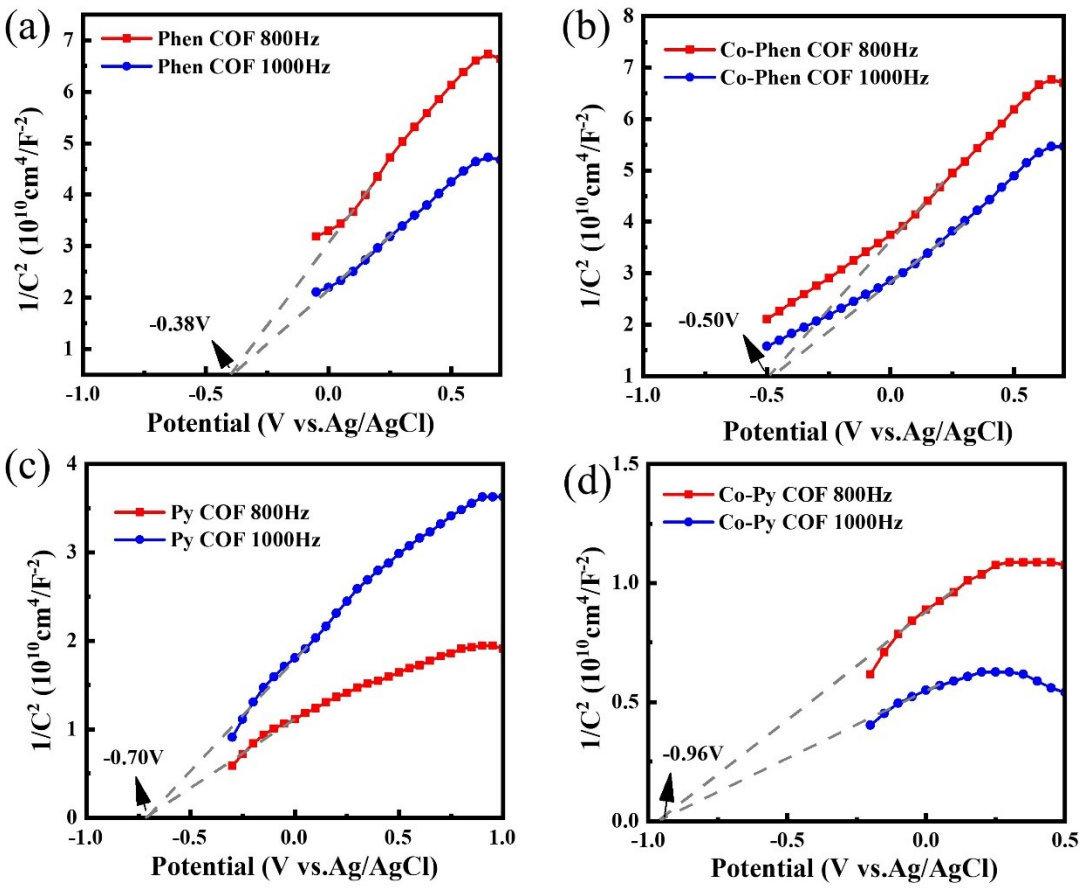

Fig. S16. Mott-Schottky plots of (a) Phen-COF, (b) Py-COF, (c) Co-Phen-COF and (d) Co-Py-COF at frequencies of 800 and 1000 Hz.

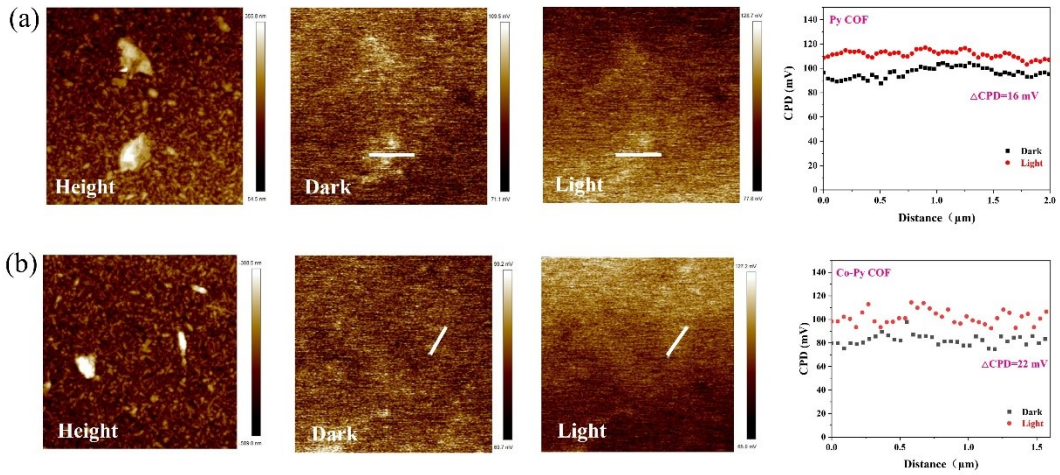

Fig. S17. Surface potential image with the KPFM of (a) Py-COF and (b) Co-Py-COF.

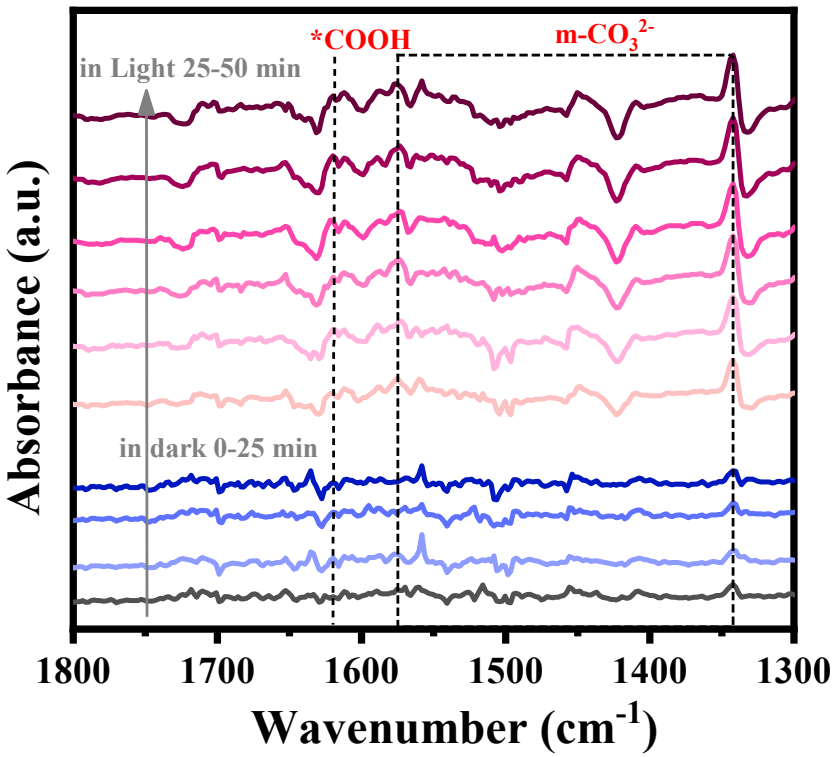

Fig. S18. An enlarged *in situ* DRIFTS spectra of CO_2 with Co-Py-COF in the range of 1800-1300 cm^{-1}.

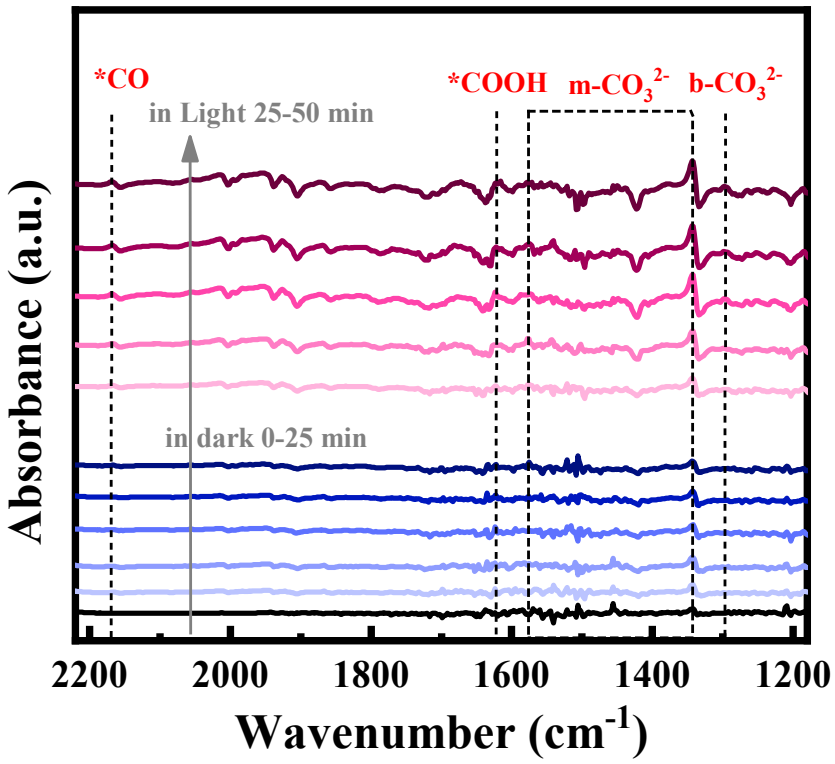

Fig. S19. *In-situ* DRIFTS spectra for Py-COF.

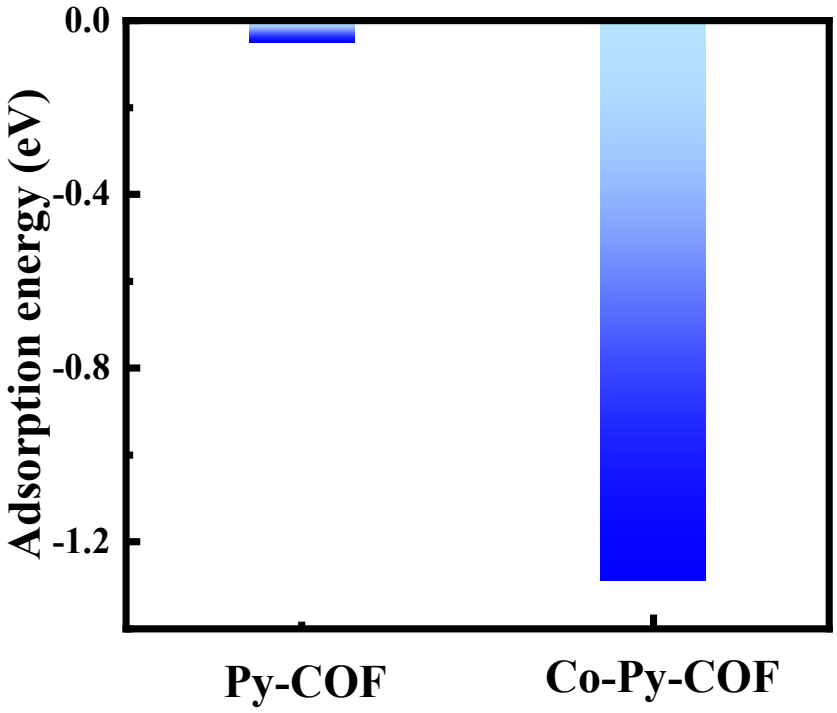

Fig. S20. CO_2 adsorption energies of Py-COF and Co-Py-COF.

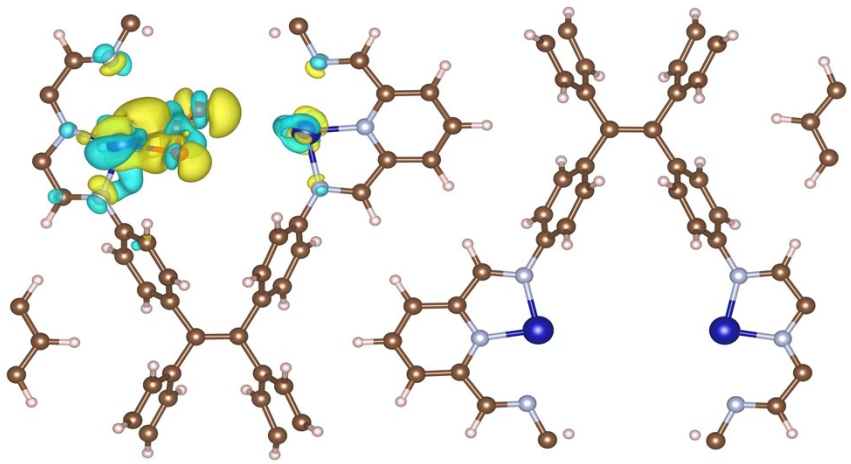

Fig. S21. The views for the charge density difference isosurfaces of Co-Py-COF@CO_2 (the cyan and yellow regions denote electron accumulation and depletion, respectively).

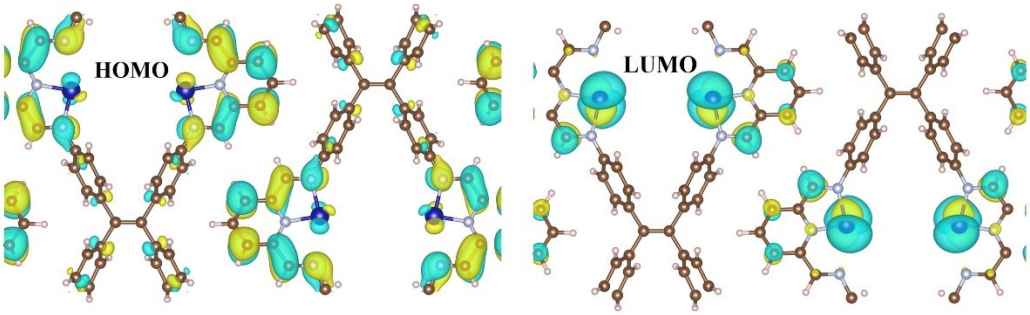

Fig. S22. Calculated HOMO-LUMO distribution of Co-Py-COF

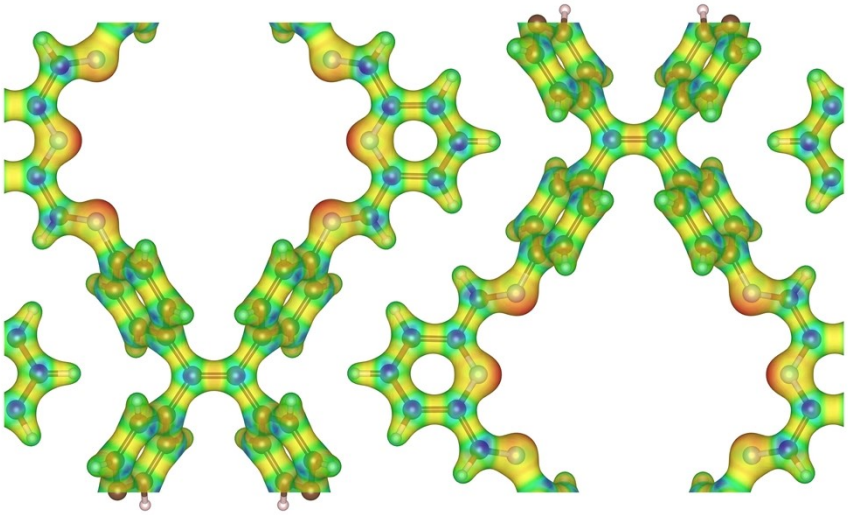

Fig. S23. Electrostatic potential map of Py-COF.

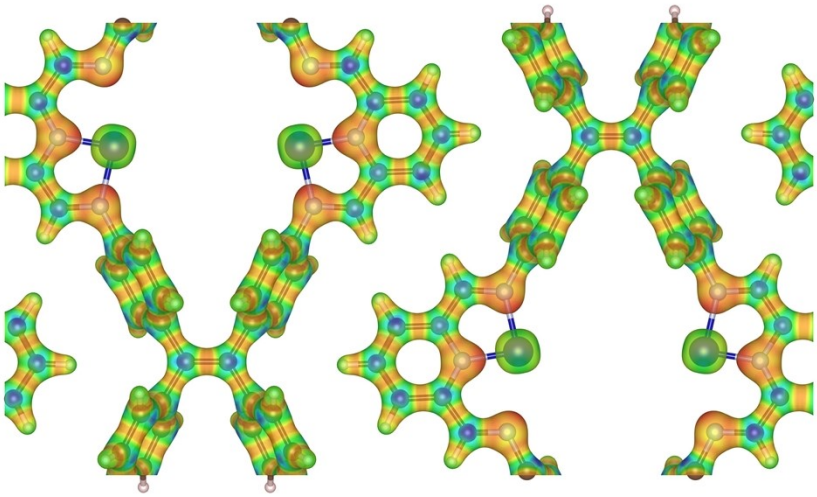

Fig. S24. Electrostatic potential map of Co-Py-COF.

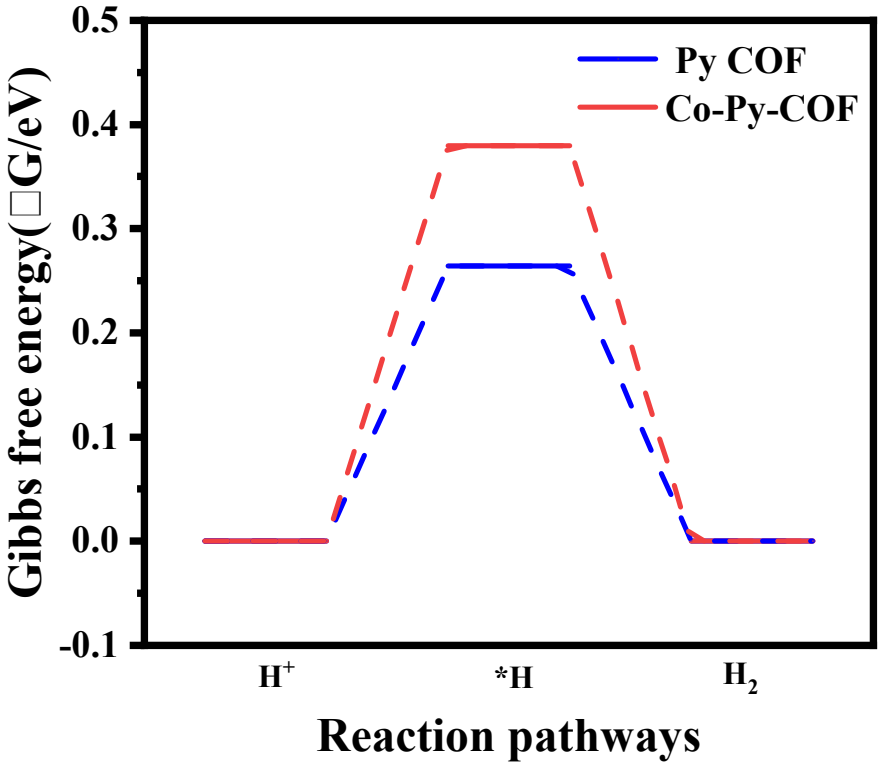

Fig. S25. Calculated Gibbs free energy profiles for HER process on Py-COF and Co-Py-COF.

Table S1. Fractional atomic coordinates for the unit cell of 1D Phen-COF.

Space group: *PMA2* a =49.38 Å b = 20.63 Å and c = 3.37 Å $\alpha = \beta = \gamma = 90°$							
Atom	x	y	z	Atom	x	y	z
N1	2.154	3.772	3.514	C27	11.093	13.959	3.219
N2	2.162	6.551	3.553	C28	10.267	13.947	4.357
N3	7.677	11.438	3.619	C29	9.143	13.129	4.443
N4	7.658	19.512	3.579	C30	8.816	12.232	3.411
N5	47.233	16.859	3.514	C31	9.668	12.188	2.289
N6	47.225	14.08	3.553	C32	10.765	13.044	2.193
N7	41.71	9.194	3.619	C33	11.092	17.01	3.206
N8	41.729	1.119	3.579	C34	10.26	17.021	4.339
N9	26.847	16.859	3.514	C35	9.13	17.833	4.416
N10	26.855	14.08	3.553	C36	8.805	18.726	3.38
N11	32.37	9.194	3.619	C37	9.663	18.77	2.262
N12	32.351	1.119	3.579	C38	10.765	17.92	2.175
N13	22.539	3.772	3.514	C39	47.205	18.188	3.636
N14	22.531	6.551	3.553	C40	48.349	18.946	3.999
N15	17.017	11.438	3.619	C41	0.151	18.291	4.23
N16	17.036	19.512	3.579	C42	0.199	16.882	4.156
C1	2.182	2.444	3.636	C43	1.392	16.155	4.459
C2	1.038	1.685	3.999	C44	1.387	14.79	4.482
C3	49.236	2.34	4.23	C45	0.189	14.062	4.203
C4	49.188	3.749	4.156	C46	0.13	12.656	4.322
C5	47.995	4.477	4.459	C47	48.326	12.001	4.107
C6	48	5.841	4.482	C48	47.188	12.755	3.714
C7	49.198	6.569	4.203	C49	48.375	14.739	3.824
C8	49.257	7.975	4.322	C50	48.38	16.201	3.801
C9	1.061	8.63	4.107	C51	42.29	0.428	2.648
C10	2.199	7.876	3.714	C52	43.517	20.298	2.907
C11	1.012	5.892	3.824	C53	44.3	20.579	4.043
C12	1.007	4.43	3.801	C54	45.494	19.905	4.265
C13	7.097	20.203	2.648	C55	45.92	18.886	3.387
C14	5.869	0.333	2.907	C56	45.119	18.571	2.279
C15	5.087	0.052	4.043	C57	43.948	19.288	2.022
C16	3.893	0.726	4.265	C58	42.288	9.869	2.686
C17	3.467	1.745	3.387	C59	43.509	10.637	2.958
C18	4.268	2.06	2.279	C60	43.946	11.649	2.077
C19	5.439	1.343	2.022	C61	45.113	12.369	2.346
C20	7.099	10.762	2.686	C62	45.903	12.056	3.463
C21	5.878	9.994	2.958	C63	45.47	11.038	4.337
C22	5.441	8.982	2.077	C64	44.279	10.361	4.103
C23	4.274	8.263	2.346	C65	38.294	6.672	3.219
C24	3.483	8.575	3.463	C66	39.12	6.684	4.357
C25	3.917	9.593	4.337	C67	40.244	7.502	4.443
C26	5.107	10.271	4.103	C68	40.571	8.399	3.411

C70	38.621	7.587	2.193	C11	24.893	3.749	4.156
C71	38.295	3.621	3.206	C11	26.085	4.477	4.459
C72	39.126	3.61	4.339	C12	26.08	5.841	4.482
C73	40.257	2.798	4.416	C12	24.883	6.569	4.203
C74	40.582	1.906	3.38	C12	24.823	7.975	4.322
C75	39.724	1.861	2.262	C12	23.632	8.63	4.107
C76	38.622	2.711	2.175	C12	22.495	7.876	3.714
C77	26.875	18.188	3.636	C12	23.681	5.892	3.824
C78	25.731	18.946	3.999	C12	23.686	4.43	3.801
C79	24.543	18.291	4.23	C12	17.597	20.203	2.648
C80	24.494	16.882	4.156	C12	18.824	0.333	2.907
C81	23.302	16.155	4.459	C12	19.606	0.052	4.043
C82	23.307	14.79	4.482	C13	20.801	0.726	4.265
C83	24.504	14.062	4.203	C13	21.226	1.745	3.387
C84	24.563	12.656	4.322	C13	20.425	2.06	2.279
C85	25.755	12.001	4.107	C13	19.255	1.343	2.022
C86	26.892	12.755	3.714	C13	17.595	10.762	2.686
C87	25.706	14.739	3.824	C13	18.816	9.994	2.958
C88	25.701	16.201	3.801	C13	19.253	8.982	2.077
C89	31.79	0.428	2.648	C13	20.419	8.263	2.346
C90	30.563	20.298	2.907	C13	21.21	8.575	3.463
C91	29.781	20.579	4.043	C13	20.777	9.593	4.337
C92	28.586	19.905	4.265	C14	19.586	10.271	4.103
C93	28.161	18.886	3.387	C14	13.6	13.959	3.219
C94	28.961	18.571	2.279	C14	14.426	13.947	4.357
C95	30.132	19.288	2.022	C14	15.551	13.129	4.443
C96	31.792	9.869	2.686	C14	15.877	12.232	3.411
C97	30.571	10.637	2.958	C14	15.025	12.188	2.289
C98	30.134	11.649	2.077	C14	13.928	13.044	2.193
C99	28.968	12.369	2.346	C14	13.601	17.01	3.206
C10	28.177	12.056	3.463	C14	14.433	17.021	4.339
C10	28.61	11.038	4.337	C14	15.563	17.833	4.416
C10	29.801	10.361	4.103	C15	15.889	18.726	3.38
C10	35.787	6.672	3.219	C15	15.031	18.77	2.262
C10	34.961	6.684	4.357	C15	13.929	17.92	2.175
C10	33.836	7.502	4.443	C15	12.347	14.799	3.181
C10	33.51	8.399	3.411	C15	12.347	16.172	3.176
C10	34.362	8.443	2.289	C15	37.04	5.832	3.181
C10	35.459	7.587	2.193	C15	37.04	4.46	3.176
C10	35.786	3.621	3.206	H1	1.105	0.597	4.058
C11	34.954	3.61	4.339	H2	48.327	1.79	4.487
C11	33.824	2.798	4.416	H3	47.086	3.917	4.694
C11	33.498	1.906	3.38	H4	47.095	6.399	4.736
C11	34.356	1.861	2.262	H5	48.352	8.524	4.596
C11	35.458	2.711	2.175	H6	1.135	9.715	4.197
C11	22.512	2.444	3.636	H7	7.478	20.244	1.602
C11	23.656	1.685	3.999	H8	5.439	19.921	4.74
C11	24.844	2.34	4.23	H9	3.293	0.48	5.144

H10	3.952	2.859	1.606	H58	28.645	17.772	1.606
H11	6.036	1.586	1.139	H59	30.73	19.046	1.139
H12	7.456	10.745	1.632	H60	32.15	9.886	1.632
H13	6.03	8.741	1.189	H61	30.724	11.89	1.189
H14	3.952	7.464	1.676	H62	28.645	13.168	1.676
H15	3.327	9.839	5.223	H63	28.02	10.792	5.223
H16	5.464	11.033	4.797	H64	30.157	9.598	4.797
H17	10.526	14.555	5.219	H65	35.22	6.076	5.219
H18	8.503	13.162	5.326	H66	33.197	7.469	5.326
H19	9.488	11.48	1.479	H67	34.182	9.152	1.479
H20	11.375	12.978	1.294	H68	36.068	7.653	1.294
H21	10.518	16.418	5.205	H69	35.211	4.213	5.205
H22	8.486	17.799	5.295	H70	33.179	2.833	5.295
H23	9.483	19.473	1.448	H71	34.176	1.158	1.448
H24	11.377	17.984	1.278	H72	36.07	2.647	1.278
H25	48.281	20.034	4.058	H73	23.588	0.597	4.058
H26	1.06	18.842	4.487	H74	25.753	1.79	4.487
H27	2.301	16.714	4.694	H75	26.995	3.917	4.694
H28	2.292	14.232	4.736	H76	26.986	6.399	4.736
H29	1.035	12.107	4.596	H77	25.728	8.524	4.596
H30	48.252	10.916	4.197	H78	23.558	9.715	4.197
H31	41.909	0.387	1.602	H79	17.215	20.244	1.602
H32	43.948	0.71	4.74	H80	19.255	19.921	4.74
H33	46.094	20.151	5.144	H81	21.4	0.48	5.144
H34	45.435	17.772	1.606	H82	20.742	2.859	1.606
H35	43.351	19.046	1.139	H83	18.657	1.586	1.139
H36	41.931	9.886	1.632	H84	17.237	10.745	1.632
H37	43.357	11.89	1.189	H85	18.663	8.741	1.189
H38	45.435	13.168	1.676	H86	20.742	7.464	1.676
H39	46.06	10.792	5.223	H87	21.367	9.839	5.223
H40	43.923	9.598	4.797	H88	19.23	11.033	4.797
H41	38.86	6.076	5.219	H89	14.167	14.555	5.219
H42	40.884	7.469	5.326	H90	16.19	13.162	5.326
H43	39.899	9.152	1.479	H91	15.205	11.48	1.479
H44	38.012	7.653	1.294	H92	13.319	12.978	1.294
H45	38.869	4.213	5.205	H93	14.176	16.418	5.205
H46	40.901	2.833	5.295	H94	16.208	17.799	5.295
H47	39.904	1.158	1.448	H95	15.21	19.473	1.448
H48	38.01	2.647	1.278	H96	13.317	17.984	1.278
H49	25.799	20.034	4.058				
H50	23.634	18.842	4.487				
H51	22.392	16.714	4.694				
H52	22.401	14.232	4.736				
H53	23.658	12.107	4.596				
H54	25.829	10.916	4.197				
H55	32.172	0.387	1.602				
H56	30.132	0.71	4.74				
H57	27.987	20.151	5.144				

Table S2. Fractional atomic coordinates for the unit cell of 1D Py-COF.

Space group: *PMA2* a =26.51 Å b = 14.82 Å and c = 5.99 Å $\alpha = \beta = \gamma = 90°$							
Atom	x	y	z	Atom	x	y	z
N1	2.906	8.541	3.248	C26	24.755	1.347	3.734
N2	1.716	11.101	3.241	C27	24.771	6.096	2.757
N3	2.901	13.652	3.195	C28	22.934	14.767	3.24
N4	23.603	6.28	3.248	C29	22.112	14.485	2.136
N5	24.793	3.72	3.241	C30	21.388	13.3	2.072
N6	23.608	1.169	3.195	C31	21.396	12.382	3.137
N7	16.161	6.28	3.248	C32	22.254	12.65	4.224
N8	14.971	3.72	3.241	C33	23.009	13.822	4.286
N9	16.156	1.169	3.195	C34	20.567	11.137	3.163
N10	10.348	8.541	3.248	C35	21.399	9.894	3.209
N11	11.538	11.101	3.241	C36	21.381	8.997	4.291
N12	10.353	13.652	3.195	C37	22.101	7.808	4.259
C1	1.029	12.2	3.588	C38	22.933	7.504	3.17
C2	26.138	12.211	3.738	C39	23.028	8.433	2.111
C3	25.414	11.077	3.388	C40	22.275	9.608	2.141
C4	26.117	9.955	2.964	C41	14.283	2.621	3.588
C5	1.015	9.991	2.967	C42	12.883	2.61	3.738
C6	1.754	13.473	3.734	C43	12.159	3.744	3.388
C7	1.738	8.725	2.757	C44	12.862	4.866	2.964
C8	3.575	0.054	3.24	C45	14.269	4.83	2.967
C9	4.397	0.336	2.136	C46	15.009	1.347	3.734
C10	5.121	1.521	2.072	C47	14.993	6.096	2.757
C11	5.113	2.439	3.137	C48	16.83	14.767	3.24
C12	4.255	2.171	4.224	C49	17.651	14.485	2.136
C13	3.5	0.999	4.286	C50	18.376	13.3	2.072
C14	5.942	3.684	3.163	C51	18.367	12.382	3.137
C15	5.11	4.927	3.209	C52	17.509	12.65	4.224
C16	5.128	5.824	4.291	C53	16.755	13.822	4.286
C17	4.408	7.013	4.259	C54	19.197	11.137	3.163
C18	3.576	7.317	3.17	C55	18.365	9.894	3.209
C19	3.481	6.388	2.111	C56	18.383	8.997	4.291
C20	4.234	5.213	2.141	C57	17.663	7.808	4.259
C21	25.48	2.621	3.588	C58	16.83	7.504	3.17
C22	0.371	2.61	3.738	C59	16.736	8.433	2.111
C23	1.096	3.744	3.388	C60	17.489	9.608	2.141
C24	0.392	4.866	2.964	C61	12.226	12.2	3.588
C25	25.495	4.83	2.967	C62	13.626	12.211	3.738

C63	14.35	11.077	3.388	H26	25.348	6.895	2.249
C64	13.647	9.955	2.964	H27	17.704	0.394	1.326
C65	12.24	9.991	2.967	H28	18.95	13.093	1.175
C66	11.501	13.473	3.734	H29	17.448	11.936	5.048
C67	11.516	8.725	2.757	H30	16.142	14.017	5.167
C68	9.68	0.054	3.24	H31	18.96	9.226	5.181
C69	8.858	0.336	2.136	H32	17.727	7.095	5.082
C70	8.134	1.521	2.072	H33	16.105	8.223	1.245
C71	8.142	2.439	3.137	H34	17.407	10.31	1.309
C72	9	2.171	4.224	H35	12.372	1.708	4.079
C73	9.754	0.999	4.286	H36	11.068	3.753	3.44
C74	7.312	3.684	3.163	H37	12.332	5.775	2.678
C75	8.144	4.927	3.209	H38	14.449	0.542	4.253
C76	8.126	5.824	4.291	H39	14.415	6.895	2.249
C77	8.846	7.013	4.259	H40	8.805	14.427	1.326
C78	9.679	7.317	3.17	H41	7.559	1.728	1.175
C79	9.774	6.388	2.111	H42	9.061	2.885	5.048
C80	9.02	5.213	2.141	H43	10.367	0.804	5.167
H1	4.449	14.427	1.326	H44	7.549	5.595	5.181
H2	5.696	1.728	1.175	H45	8.782	7.726	5.082
H3	4.194	2.885	5.048	H46	10.404	6.598	1.245
H4	2.888	0.804	5.167	H47	9.102	4.511	1.309
H5	5.706	5.595	5.181	H48	14.137	13.113	4.079
H6	4.472	7.726	5.082	H49	15.441	11.068	3.44
H7	2.851	6.598	1.245	H50	14.177	9.046	2.678
H8	4.153	4.511	1.309	H51	12.06	14.279	4.253
H9	25.627	13.113	4.079	H52	12.094	7.926	2.249
H10	24.323	11.068	3.44				
H11	25.586	9.046	2.678				
H12	1.195	14.279	4.253				
H13	1.161	7.926	2.249				
H14	22.06	0.394	1.326				
H15	20.814	13.093	1.175				
H16	22.316	11.936	5.048				
H17	23.621	14.017	5.167				
H18	20.803	9.226	5.181				
H19	22.037	7.095	5.082				
H20	23.659	8.223	1.245				
H21	22.357	10.31	1.309				
H22	0.882	1.708	4.079				
H23	2.186	3.753	3.44				
H24	0.923	5.775	2.678				
H25	25.314	0.542	4.253				

Table S3. N_2 adsorption-desorption and CO_2 physisorption results of Py-COF and Co-Py-COF.

Sample	S_{BET} ($m^2\ g^{-1}$) [(a)]	V_{Tot} ($cm^3\ g^{-1}$) [(b)]	CO_2 ($cm^3\ g^{-1}$)
Py-COF	447.0	1.00	23.2
Co-Py-COF	430.9	0.95	35.8

[(a)] Specific surface area measured by BET model;

[(b)] The total pore volume measured at P/P0=0.99.

Table S4. EXARF fitting parameters at the Co K-edge for Co-Py-COF.

Sample	Shell	*CN*	*R*(Å)	σ^2(Å^2)	$\triangle E_0$(eV)	*R* factor
Co-Py-COF	Co-N/O	4±0.8	2.06±0.01	0.015±0.003	0.35	0.011

CN, coordination number; *R*, distance between absorber and backscatter atoms; σ^2, Debye-Waller factor (a measure of thermal and static disorder in absorber-scatterer distances); $\triangle E_0$ is an edge-energy shift (the difference between the zero-kinetic energy value of the sample and that of the theoretical model).

Table S5. The performance comparison of COF-based photocatalysts for photocatalytic CO_2 reduction.

Photocatalyst	Photosensitizer	Light Condition	Production rate for CO (μmol g^{-1} h^{-1})	References
TAPBB-COF	-	300 W Xe lamp	24.6	[1]
Mo-COF	-	300 W Xe lamp ($\lambda \geq 420$ nm)	6.2	[2]
TTCOF-Zn	-	300 W Xe lamp ($\lambda \geq 420$ nm)	2.1	[3]
MAF-34-CoRu	-	300 W Xe lamp ($\lambda \geq 420$ nm)	5.43	[4]
N-ZnO/TAPT-DMTP COF	-	300 W Xe lamp	2.4	[5]
UJN-1	-	300 W Xe lamp ($\lambda \geq 400$ nm)	28.7	[6]
1.0% Ni-tp-COF	-	300 W Xe lamp (AM 1.5)	15	[7]
CoPor-RuN_3 COP	-	300 W Xe lamp ($\lambda \geq 400$ nm)	37.1	[8]
BTT-bpy-COF-Re	-	300 W Xe lamp ($\lambda \geq 400$ nm)	110.9	[9]
Re^{I}bpyDBC	-	300 W Xe lamp ($\lambda \geq 420$ nm)	180	[10]
Co-Py-COF	-	300 W Xe lamp ($\lambda \geq 420$ nm)	21.7	This work
Co-Py-COF	$[Ru(bpy)_3]Cl_2$	300 W Xe lamp ($\lambda \geq 420$ nm)	3310	This work
Fe SAS/Tr-COFs	$[Ru(bpy)_3]Cl_2$	300 W Xe lamp ($\lambda \geq 420$ nm)	980.3	[11]
TFBD-COF-Co-SA	$[Ru(bpy)_3]Cl_2$	300 W Xe lamp ($\lambda \geq 420$ nm)	1480	[12]
DQTP-COF-Co	$[Ru(bpy)_3]Cl_2$	300 W Xe lamp	1020	[13]
JUC-640-Co	$[Ru(bpy)_3]Cl_2$	300 W Xe lamp	15.14	[14]
COF-RuBpy-Co	$[Ru(bpy)_3]Cl_2$	300 W Xe lamp	2190	[15]

Table S6. The bond lengths and angles of CO_2 adsorbed on COFs.

	C-O bond lengths (Å)	bond angles (°)
Single CO_2	1.18	180
CO_2 adsorbed on Py-COF	1.18	177.14
CO_2 adsorbed on Co-Py-COF	1.28/ 1.21	139.28

3. Reference

[1] L. Wang, R. Wang, X. Zhang, J. Mu, Z. Zhou, Z. Su, Improved photoreduction of CO_2 with water by tuning the valence band of covalent organic frameworks, ChemSusChem 13 (2020) 2973-2980.

[2] M. Kou, W. Liu, Y. Wang, J. Huang, Y. Chen, Y. Zhou, Y. Chen, M. Ma, K. Lei, H. Xie, Photocatalytic CO_2 conversion over single-atom MoN_2 sites of covalent organic framework, Appl. Catal. B-Environ. 291 (2021) 120146.

[3] M. Lu, J. Liu, Q. Li, M. Zhang, M. Liu, J. L. Wang, D. Q. Yuan, Y. Q. Lan, Rational design of crystalline covalent organic frameworks for efficient CO_2 photoreduction with H_2O, Angew. Chem. Int. Ed. 58 (2019) 12392-12397.

[4] N.-Y. Huang, J. Shen, X. Zhang, P. Liao, J. Zhang, X. Chen, Coupling ruthenium bipyridyl and cobalt imidazolate units in a metal-organic framework for an efficient photosynthetic overall reaction in diluted CO_2, J. Am. Chem. Soc. 144 (2022) 8676-8682.

[5] M. Mu, L. Meng, S. Ma, W. Chen, X. Yin, G. Bai, Interfacial imine-bridging and charge directional migration dual regulation of ZnO/covalent organic frameworks S-scheme heterostructure for boosting photocatalytic CO_2 reduction, J. Colloid Interf. Sci. 686 (2025) 63-74.

[6] S. Li, C. Gao, H. Yu, Y. Wang, S. Wang, W. Ding, L. Zhang, J. Yu, Vinylene-linked donor-π-acceptor metal-covalent organic framework for enhanced photocatalytic CO_2 reduction, Angew. Chem. Int. Ed. 63 (2024) e202409925.

[7] P. Wang, Y. Dai, Z. Song, Y. Wang, J. Wei, Z. Liu, Y. Ma, F. Yang, J. Qu, S. Liu, Y. Cai, X. Yang, C. Li, J. Hu, Polarized microenvironment-modulated covalent organic frameworks with nickel single atoms for enhanced CO_2 photoreduction, Chem. Eng. J. 511 (2025) 162084.

[8] S. Chen, P. Kong, H. Niu, H. Liu, X. Wang, J. Zhang, R. Li, Y. Guo, T. Peng, Co-porphyrin/Ru-pincer complex coupled polymer with Z-scheme molecular

junctions and dual single-atom sites for visible light-responsive CO_2 reduction, Chem. Eng. J 431 (2022) 133357.

[9] H. Dong, H. Chen, L. Bai, N. Zhang, Y. Tian, B. Li, Y. Wang, X. Zhang, F. Zhang, Benzotrithiophene-based covalent organic frameworks with rhenium modified for artificial photosynthetic CO2 reduction, Inorg. Chem. 63 (2024) 24421-24428.

[10] L. Spies, M. E. G. Carmo, M. Döblinger, Z. Xu, T. Xue, A. Hartschuh, T. Bein, J. Schneider, A. O. T. Patrocinio, Designing atomically precise and robust COF hybrids for efficient photocatalytic CO_2 reduction, Small 21 (2025) 2500550.

[11] L. Ran, Z. Li, B. Ran, J. Cao, Y. Zhao, T. Shao, Y. Song, M. Leung, L. Sun, J. Hou, Engineering single-atom active sites on covalent organic frameworks for boosting CO_2 photoreduction, J. Am. Chem. Soc. 144 (2022) 17097-17109.

[12] Y. Yang, Y. Lu, H. Zhang, Y. Wang, H. Tang, X. Sun, G. Zhang, F. Zhang, Decoration of active sites in covalent−organic framework: an effective strategy of building efficient photocatalysis for CO_2 reduction, ACS Sustainable. Chem. Eng. 9 (2021) 13376.

[13] M. Lu, Q. Li, J. Liu, F. Zhang, L. Zhang, J. Wang, Z. Kang, Y. Lan, Installing earth-abundant metal active centers to covalent organic frameworks for efficient heterogeneous photocatalytic CO_2 reduction, Appl. Catal. B: Environ. 254 (2019) 624-633.

[14] J. Ding, X. Guan, J. Lv, X. Chen, Y. Zhang, H. Li, D. Zhang, S. Qiu, H. Jiang, Q. Fang, Three-dimensional covalent organic frameworks with ultra-large pores for highly efficient photocatalysis, J. Am. Chem. Soc. 145 (2023) 3248-3254.

[15] L. Gong, L. Liu, S. Zhao, S. Yang, D. Si, Q. Wu, Q. Wu, Y. Huang, R. Cao, Rapid charge transfer in covalent organic framework via through-bond for enhanced photocatalytic CO2 reduction, Chem. Eng. J. 458 (2023) 141360.